© 2015. Published by The Company of Biologists Ltd | Development (2015) 142, 2696-2703 doi:10.1242/dev.122044

RESEARCH ARTICLE

Yap and Taz are required for Ret-dependent urinary tract morphogenesis

Antoine Reginensi[1,*], Masato Hoshi[2], Sami Kamel Boualia[3], Maxime Bouchard[3], Sanjay Jain[2] and Helen McNeill[1,4,*]

ABSTRACT

Despite the high occurrence of congenital abnormalities of the lower urinary tract in humans, the molecular, cellular and morphological aspects of their development are still poorly understood. Here, we use a conditional knockout approach to inactivate within the nephric duct (ND) lineage the two effectors of the Hippo pathway, *Yap* and *Taz*. Deletion of *Yap* leads to hydronephrotic kidneys with blind-ending megaureters at birth. In *Yap* mutants, the ND successfully migrates towards, and contacts, the cloaca. However, close analysis reveals that the tip of the $Yap^{-/-}$ ND forms an aberrant connection with the cloaca and does not properly insert into the cloaca, leading to later detachment of the ND from the cloaca. *Taz* deletion from the ND does not cause any defect, but analysis of $Yap^{-/-};Taz^{-/-}$ NDs indicates that both genes play partially redundant roles in ureterovesical junction formation. Aspects of the $Yap^{-/-}$ phenotype resemble hypersensitivity to RET signaling, including excess budding of the ND, increased phospho-ERK and increased expression of *Crlf1*, *Sprouty1*, *Etv4* and *Etv5*. Importantly, the $Yap^{ND-/-}$ ND phenotype can be largely rescued by reducing *Ret* gene dosage. Taken together, these results suggest that disrupting *Yap*/*Taz* activities enhances Ret pathway activity and contributes to pathogenesis of lower urinary tract defects in human infants.

KEY WORDS: Yap, Taz, Ret, Nephric duct, CAKUT, Lower urinary tract

INTRODUCTION

Congenital abnormalities of the kidney and urinary tract (CAKUT) are among the most common birth defects in humans. They encompass a spectrum of structural and functional kidney and urinary tract defects, including renal agenesis, duplex kidneys, megaureter, hypoplasia and multicystic dysplasia, which arise from defects during development (Schedl, 2007). A large proportion of CAKUT patients show a failure to properly connect the ureter to the bladder, a connection known as the ureterovesical junction (UVJ). Defective UVJ formation results in obstruction of urine flow into the bladder, causing dilation of the ureter (known as hydroureter or megaureter) and/or the renal pelvis (hydronephrosis), or reflux of urine from the bladder into the ureter and kidneys (vesicoureteral reflux). Despite the high occurrence of lower urinary tract abnormalities in humans, the molecular, cellular and morphological aspects underlying UVJ formation are still poorly understood.

The first step in the formation of a working urinary system is the formation of the nephric duct (ND), which extends towards the posterior part of the embryo to join the cloaca (bladder-urethra primordium) by E9.5 (Fig. 1A). An outgrowth from the caudal end of the ND, known as the ureteric bud (UB), grows towards the metanephric mesenchyme (MM) at E10.5. The portion of the UB that lies outside the MM will form the ureter, a tube that will connect the kidney with the bladder. At E10.5, the UB is connected indirectly to the cloaca via the common nephric duct (CND), the most caudal segment of the ND. In order to be functional, the ureters need to rearrange to insert directly into the bladder primordium, through a process called ureter-bladder maturation that occurs between E11 and E14.5. This process requires the apoptotic elimination of the CND and the growth of the bladder to enable the separation of the distal end of the ureter from the ND, and migration to its final position within the bladder (Fig. 1A and Uetani et al., 2009).

Although the molecular and cellular origin of CAKUT anomalies in humans are poorly understood, mutational analyses in mice have identified a number of genes involved in proper formation of the kidney and urinary tract [reviewed by Uetani and Bouchard (2009)]. A crucial signaling pathway for the development of the urinary system is the Gdnf/Ret pathway. Mutations in the tyrosine kinase receptor *Ret*, or in genes that control Ret expression or signaling, result in delay or failure of the ND to insert into the cloaca (Chia et al., 2011; Hoshi et al., 2012; Weiss et al., 2014). Ret signaling is also crucial for the sprouting of the UB and its branching morphogenesis. Positioning of the UB along the ND is crucial for normal morphogenesis. Indeed, in *Gata2* hypomorphic (Hoshino et al., 2008) and *Bmp4* heterozygous (Miyazaki et al., 2000) mutants, the lower end of the ureter does not reach the bladder, due to a more rostral budding site. Improper urinary tract development is also observed as a consequence of defective ureter maturation. This process, which relies on apoptotic removal of the CND, requires the Ptprs and Ptprf phosphatases (Uetani et al., 2009), EphA4/EphA7 signaling (Weiss et al., 2014), retinoic acid and Ret-MAPK signaling (Chia et al., 2011; Batourina et al., 2002, 2005; Hoshi et al., 2012) and the expression of Discs, large homolog 1 (Dlg1) (Iizuka-Kogo et al., 2007). Thus, strict regulation of apoptosis, proliferation, cell migration and cell adhesion are all needed to form a functional urinary system.

The Hippo pathway is a highly conserved kinase cassette that regulates tissue growth, cell fate and regeneration in metazoans by controlling the activity of its two downstream effectors Yap and Taz [reviewed by Staley and Irvine (2012); Zhao et al. (2008); Halder and Johnson (2011)]. Yap and Taz are closely related transcriptional co-regulators that control expression of pro-proliferative and anti-apoptotic genes. When the Hippo kinases Mst and Lats are

[1]Lunenfeld–Tanenbaum Research Institute, Mount Sinai Hospital, Toronto, Canada M5G 1X5. [2]Departments of Internal Medicine (Renal Division) and Pathology, Washington University School of Medicine, St. Louis, MO 63110, USA. [3]Goodman Cancer Research Centre and Department of Biochemistry, McGill University, Montreal, Canada H3A 1A3. [4]Department of Molecular Genetics, University of Toronto, Toronto, Canada M5G 1X5.

*Authors for correspondence (reginensi@lunenfeld.ca; mcneill@lunenfeld.ca)

Received 12 January 2015; Accepted 23 June 2015

Development (2015) 142, 2696-2703 doi:10.1242/dev.122044

active, Yap and Taz are phosphorylated and excluded from the nucleus. Loss of Hippo signaling leads to unrestricted proliferation in flies and mammals and has been linked to a variety of cancers [reviewed by Pan (2010); Harvey and Tapon (2007)]. *Yap* knockout (*Yap*$^{-/-}$) embryos die at embryonic day (E)8.5 (Morin-Kensicki et al., 2006), and both *Yap* and *Taz* are essential for nephrogenesis (Hossain et al., 2007; Makita et al., 2008; Reginensi et al., 2013), but their role in lower urinary tract morphogenesis remains unknown. Here, we examine the effects of loss of *Yap* and *Taz* in the development of the lower urinary tract, and demonstrate that *Yap* and *Taz* play crucial and partially redundant roles in establishing ureter-bladder connectivity, via the control of cell organization and regulation of the activity of the Ret signaling pathway.

RESULTS

CAKUT in *Yap* ND mutants

To assess the function of *Yap* in urinary tract development, we removed *Yap* from the ND using the *Hoxb7:Cre* line (Zhao et al., 2004). The *Hoxb7* promoter drives Cre recombinase expression in the ND as early as E9 and in all epithelial structures derived from the UB, but not in the cloaca epithelium (Zhao et al., 2004). We found that *Hoxb7:Cre*$^{tg/+}$ *Yap*$^{flox/flox}$ (termed *Yap*$^{ND-/-}$) newborns were obtained at Mendelian ratios; however, despite successful feeding, >90% of *Yap*$^{ND-/-}$ animals died within 24 h after birth. Gross anatomical examination revealed that neonatal (P0) *Yap*$^{ND-/-}$ animals had a variety of severe anomalies of the kidney and the urinary tract with empty bladders (Fig. 1B-D). Histological examination of P0 kidney sections revealed severe kidney anomalies, including duplicated renal system, hydroureter, blind-ending ureter and hydronephrosis (Fig. 1B′-D′). Quantification revealed that 90% of *Yap*$^{ND-/-}$ mutants (34/38 kidneys) had hydroureter, combined with 69% (26/38) hydronephrosis and 37% duplicated renal systems (14/38) (Fig. 1E). The remaining four kidneys (10%) were small and dysplastic. Only 2% of *Yap*$^{ND-/-}$ pups (6/277 pups) survived to weaning, with severely dysplastic and hydronephrotic kidneys (supplementary material Fig. S1A-C). These rare survivors are probably due to less-efficient Cre excision (supplementary material Fig. S1D-F′). Overall, our data demonstrate that Yap plays a crucial role in the *Hoxb7* lineage for correct development of the urinary tract.

Yap is essential for formation of the ureter-bladder junction

Hydroureter/nephrosis arises from defective flow of urine from the kidney to the bladder, which could be due to functional or physical obstruction. To determine whether a physical obstruction contributed to hydroureter/nephrosis in *Yap*$^{ND-/-}$ mutants, we performed intrapelvic dye injections on E18.5 controls and *Yap*$^{ND-/-}$ embryos. In controls, dye flowed down the ureter into the bladder, where it could be easily detected within five minutes (n=3, Fig. 1F). By contrast, in *Yap*$^{ND-/-}$ mice, intrapelvic injected dye was never detected in the bladder (n=3, Fig. 1G). Moreover, histological analysis before urine production (E14.5) reveals that *Yap* deletion leads to hypodysplastic kidneys but no hydroureter (supplementary material Fig. S1G,H), consistent with the hypothesis that the production of urine leads to the observed hydroureter. Hydronephrosis can also be caused by defects in the smooth muscle layer (Airik et al., 2006); however, staining with antibodies against alpha-smooth muscle actin demonstrated that *Yap* deletion from the ureter does not affect the smooth muscle layer of the ureter at E16.5 (supplementary material Fig. S1I,J).

To obtain more insight into the developmental defects of *Yap*$^{ND-/-}$ mutants, we dissected P0 urinary tracts. Strikingly, 85%

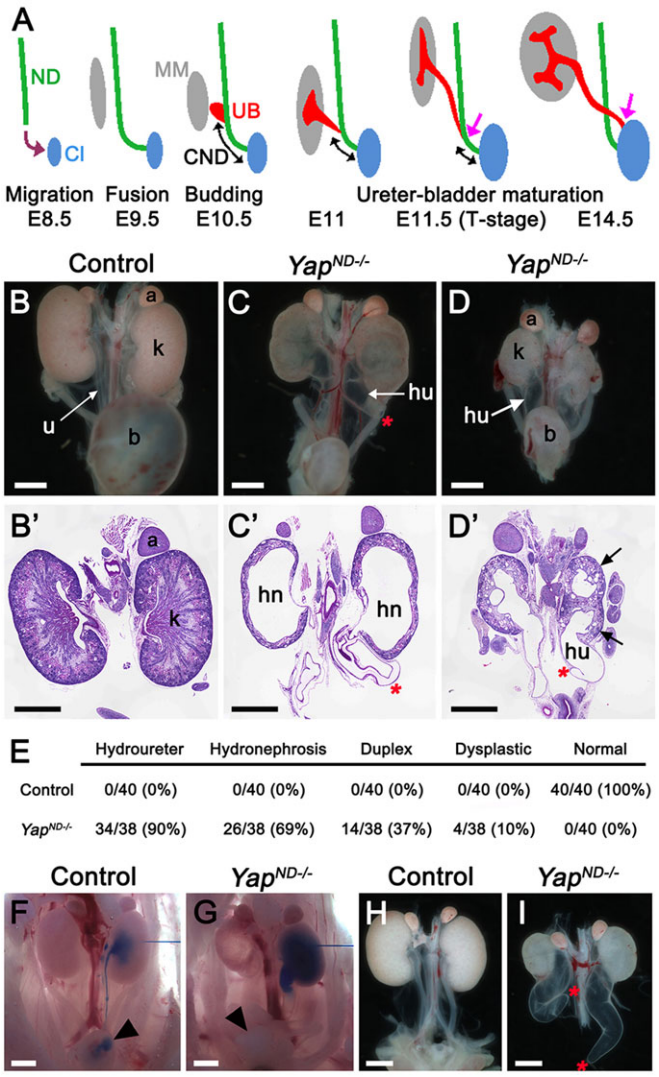

Fig. 1. CAKUT in *Yap* mutants. (A) Diagram of urinary tract development and ureter-bladder maturation. ND, nephric duct; Cl, cloaca; CND, common nephric duct; UB, ureteric bud; MM, metanephric mesenchyme. (B-D) Macroscopic views of the urogenital system in wild-type and *Yap*$^{ND-/-}$ kidneys at P0. Note bilateral reduction in kidney size, dilated ureter and empty bladder in mutant animals compared with control. PAS staining on kidneys of P0 wild-type (B′) and *Yap*$^{ND-/-}$ animals (C′,D′) showed the duplicated system (black arrows in D′), hydroureter (hu) and hydronephrosis (hn) in mutant embryos. (E) Quantification of kidney and urinary tract anomalies in controls and *Yap*$^{ND-/-}$ mutants. (F,G) Intrapelvic blue ink injection revealed physical obstruction in *Yap* mutants at E18.5. (H,I) Macroscopic view of the urogenital system from wild type and *Yap* mutant at E18.5 showed blind-ending ureter (red asterisks) in *Yap* mutant, whereas the ureter is connected to the bladder in the control (bladders were dissected out to visualize ureters better). A, adrenal gland; b, bladder; k, kidney; u, ureter. Scale bars: 1 mm.

of kidneys (16/19) displayed a blind-ending ureter in *Yap* cKO kidneys, whereas in controls, ureters were always connected to the bladder (Fig. 1H,I). Taken together, these data indicate that hydroureter/nephrosis seen in *Yap* cKO embryos is due to physical obstruction of urine flow to the bladder.

Yap signaling is required for ND insertion into the cloaca and lower urinary tract morphogenesis

The blind-ending ureter phenotype observed in *Yap* mutants could result from the inability of the ND to reach the cloaca, as seen in *Ret*,

Development (2015) 142, 2696-2703 doi:10.1242/dev.122044

Gata3 and *Raldh2* (*Aldh1a2* – Mouse Genome Informatics) mutants (Chia et al., 2011). To address this hypothesis, we examined earlier stages of kidney development. Surprisingly, whole-mount-*in situ* hybridization (WM-ISH) analysis with *Pax2* riboprobes at E9.5 revealed that the NDs of controls and *Yap* mutant embryos had elongated successfully along the anteroposterior axis and turned to reach the cloacal epithelium (supplementary material Fig. S2A,B), thus indicating that ND elongation towards the cloaca is independent of *Yap* function.

We examined with higher resolution the ND-cloaca connection point using whole-mount-immunofluorescence (WM-IF) analysis at E10.5. We used Pax2 to mark the ND and the MM, and E-cadherin to mark the ND and the cloaca. This analysis confirmed that the $Yap^{ND-/-}$ ND reached, and came in contact with, the cloaca epithelium (see supplementary material Fig. S2C-E for low-magnification view). However, the morphology of the ND-cloaca connection was highly abnormal in *Yap* mutants. Whereas the tip of the ND formed a smooth connection with the cloaca in wild type (Fig. 2A), *Yap* mutant NDs consistently formed an aberrant connection, with the most distal tip not adhering to the cloaca, and often extending beyond the cloacal surface (Fig. 2B,C).

To determine whether the ND properly inserts into the cloaca, we conducted Pax2 and E-cadherin WM-IF at E11.25 in controls and *Yap* mutants. In controls, a single UB underwent the first branching event to reach the T-stage, and the ND was connected to the cloaca via a relatively short CND (Fig. 2D, Fig. 3A; quantification in supplementary material Fig. S3D, average length of CND in controls=178±18 µm s.d.; *n*=8). In *Yap* mutants, a second (or more) UB was often observed anterior to the primary bud (arrow in Fig. 2E, Fig. 3F,G; supplementary material S2F,G), the average length of the CND was increased (Fig. 3A-C; quantification in supplementary material Fig. S3D, mean $Yap^{ND-/-}$ CND length=313±51 µm s.d.; *n*=10), and the ND connection to the cloaca was always abnormal. Either a thin 'bridge' of cells remained as a connection between the ND and the cloaca (Fig. 2E,E′,H; supplementary material Fig. S2F-G′), or the ND was not connected to the cloaca (Fig. 2F and Fig. 3B).

Further analysis revealed that the ND contacts the cloaca epithelium, but the ND does not properly insert into it. As development progressed in *Yap* mutants, Pax2/E-cadherin double-immunostaining revealed that the ND appears to retract away from the cloaca with a concomitant extension of cloacal epithelial cells as early as E11, before ureter remodeling occurs (Fig. 2E′,H;

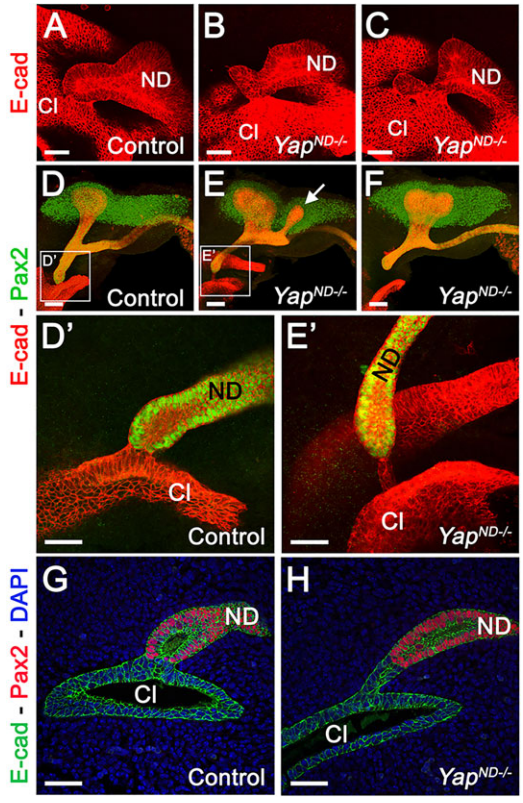

Fig. 2. *Yap* is essential for ND insertion into the cloaca. (A-C) High-magnification views of the ND-cloaca connection at E10.5 using E-cadherin WM-IF showed an abnormal connection of the ND with the cloaca in mutants compared with controls (low-magnification views are shown in supplementary material Fig. S2C-E). (D-E′) Pax2/E-cadherin WM-IF staining at E11.5. (D′,E′) Higher-magnification views of the ND-cloaca connection shown in D and E. (G,H) Pax2/E-cadherin staining of the ND-cloaca connection on tissue sections. ND, nephric duct; Cl, cloaca. Scale bars: 50 µm in A-C,D′,E′,G,H; 100 µm in D-F.

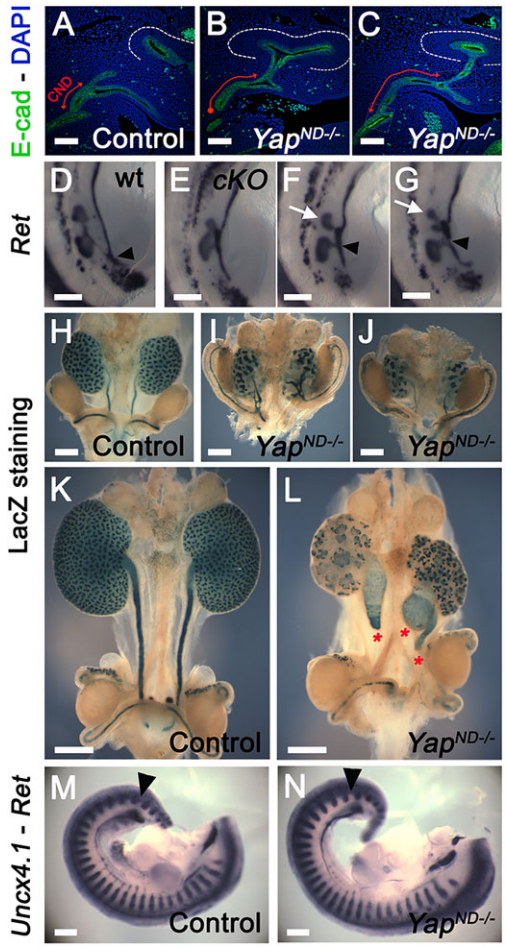

Fig. 3. Increased CND length and defective ureter-bladder maturation in *Yap* mutants. (A-C) Confocal images of E-cadherin staining at E11.5 revealed the increase in the CND length (red double arrows) and ND-cloaca disconnection in the mutants compared with controls. (D-G) WM-ISH using *Ret* probe at E11.5 showed formation of supernumerary UBs in *Yap* mutants (white arrows in F and G) compared with controls. (H-L) β-galactosidase staining of the urogenital tract at E14.5 and E16.5 revealed abnormal branching pattern and blind-ending ureter (red asterisks) in *Yap* mutants. (M,N) Double WM-ISH using *Ret* and *Uncx4.1* riboprobes showed that the UB sprouts (black arrowheads) in both genotypes between the 26th and 27th somites. Scale bars: 100 µm in A-C; 250 µm in D-G,M,N; 500 µm in H-L.

Development (2015) 142, 2696-2703 doi:10.1242/dev.122044

supplementary material Fig. S2G,G′). The normal continuity of ND and cloaca lumens does not occur in *Yap* mutants. Analysis of E12.5 embryos confirmed defective ureter-bladder maturation in *Yap* mutants, with defective ND-cloaca connection and CND elimination (supplementary material Fig. S3A-C). In wild-type animals, the length of the CND is 139±8 µm s.d. at E12.5, whereas in *Yap* mutants, we observed an increase in CND length at E12.5 (472±71 µm s.d.; n=6; supplementary material Fig. S3A-D). In order to visualize the developing urinary tract better at later stages, we crossed the *Rosa26-fl-Stop-fl-lacZ* reporter allele into control and $Yap^{ND-/-}$ genetic backgrounds and stained urogenital tracts for β-galactosidase activity. As the *Hoxb7* promoter does not drive Cre expression in the cloaca, this structure is not visualized with this technique. β-galactosidase staining at E14.5 and E16.5 showed a regular UB branching pattern, and ureters that separated from the ND to insert into the bladder wall in controls (Fig. 3H,K). By contrast, $Yap^{ND-/-}$ kidneys had a reduced and abnormal branching, with ureters still connected to the ND at E14.5 (Fig. 3I,J) and ending blindly at E16.5 (Fig. 3L).

Increased proliferation in *Yap* mutant CND

The increased length of the CND observed in *Yap* mutant embryos could be due to a rostral UB budding, which impairs proper formation of the later ureter-bladder connection. Alternatively, altered proliferation or apoptosis might lead to defects in formation of this connection. To test whether *Yap* deletion affects the site of the primary bud along the ND, we performed double WM-ISH analysis with both *Ret* (ND and UB) and *Uncx4.1* (posterior half of developing somites) riboprobes at E11. In both wild type and $Yap^{ND-/-}$ mutants, the UB sprouted from the ND between the 26th and 27th somites (Fig. 3M,N), indicating that *Yap* deletion does not impact the position of the primary UB along the ND.

An alternative explanation for the increased CND length observed in *Yap* mutants would be a reduction in apoptosis in the CND. Apoptosis is crucial for ureter-bladder maturation, as the CND must undergo controlled apoptosis in order to bring the distal end of the ureter in contact with the bladder. To test this hypothesis, we performed cleaved-caspase 3 and terminal deoxynucleotidyl transferase dUTP nick end labeling (TUNEL) staining in control and $Yap^{ND-/-}$ kidneys at different timepoints. Interestingly, we found comparable rates of apoptosis in control and *Yap* cKO CND at E11.5 (Fig. 4A-C′) and E12 (supplementary material Fig. S4A-E). Loss of *Yap* is predicted to increase apoptosis and reduce proliferation; however, even at earlier timepoints (E11, Fig. 4D-I′), using both TUNEL and cleaved-caspase 3 approaches, we found that *Yap* deletion does not lead to increased apoptosis in the CND. Interestingly, the characteristic bridging structure observed in *Yap* mutants does undergo apoptosis, as seen by TUNEL and cleaved-caspase 3-positive staining in the E-cadherin structure between the arrows and the cloaca (Fig. 4F-G′). Later, at E13.5, there was a sixfold increase in apoptosis in *Yap* cKO in the ureter (Fig. 4J-L). Then, defective ureter remodeling observed in *Yap* mutants is not due to major defect in inducing CND elimination by apoptosis.

Finally, elongation of the CND can be the result of increased proliferation. We examined proliferation using BrdU incorporation into the CND at E11.5. Very limited proliferation was observed in control CND (4.96%±1.5, n=10). Surprisingly, proliferation increased 2.6-fold in $Yap^{ND-/-}$ CND (13.07%±4.9, n=10; Fig. 4M-O). This increase in proliferation could explain the increase in CND length.

Cell specification and cell polarity are not eliminated by loss of *Yap* in the ND

Several genes have been implicated in ureter-bladder maturation, affecting either migration of the ND (*Gata3*, *Raldh2*, *Ret*), UB sprouting position (*Gata2*, *Bmp4*), formation of a single UB (*Gata3*, *Ret*, *Slit2*, *Robo2*, *Sprouty1*, *Islet1*; see Grieshammer et al., 2004; Basson et al., 2005; Kaku et al., 2013; Hoshi et al., 2012; Jain et al., 2006), defective CND elimination by apoptosis (*Rar*, *Ptprs;Ptprf*, *RetY1015F*, *Dlgh1*) or defective adhesion between the ND and the

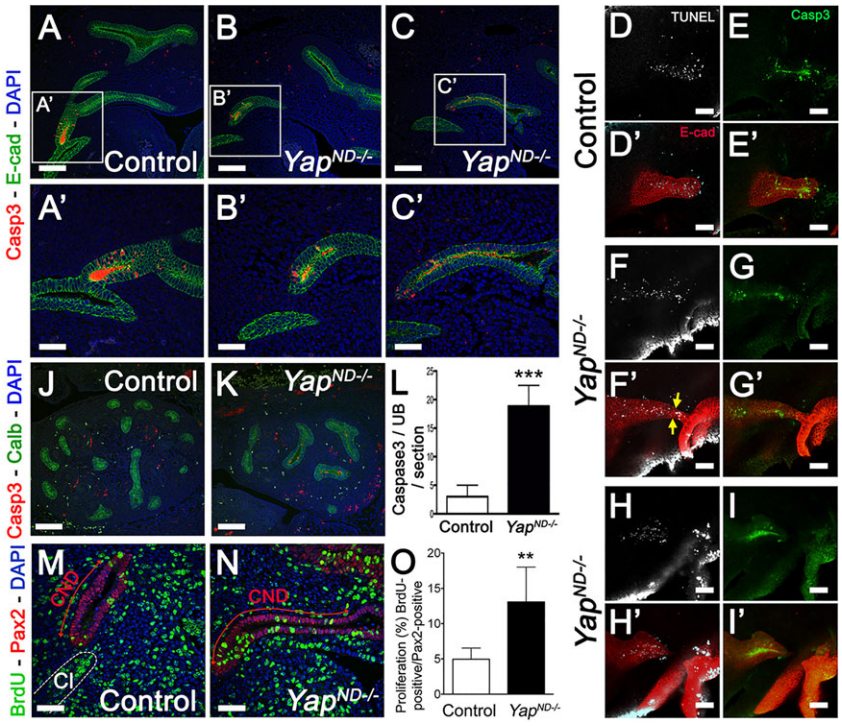

Fig. 4. Compared with controls, *Yap* mutants have increased proliferation in early CND but only show increased apoptosis at E13.5. (A-C′) Low- and high-magnification views of confocal analysis of apoptosis in the CND using anti-cleaved-caspase 3 antibody revealed similar CND apoptosis rates in controls and mutants at E11.5. (D-I′) Analysis of TUNEL and cleaved-caspase 3 in E11 CND in control (D-E′) and *Yap* mutants (F-I′). E-cadherin counterstaining was used to label the epithelial structures. (J,K) Cleaved-caspase 3 staining at E13.5 kidneys. Co-staining with anti-calbindin antibody was used to stain the *Yap*-depleted ureter compartment. (L) Quantitative analysis of the number of cleaved-caspase 3 staining revealed a significant increase in cell death (***P<0.0001) in *Yap* mutants compared with controls at E13.5. (M,N) Confocal images of BrdU incorporation in CND cells at E11.5. Co-staining with anti-Pax2 antibody and DAPI was used to label the CND (red double arrows) and identify the cloaca (white dashed line in M). (O) Quantitative analysis of BrdU incorporation showed an increase in the percentage of $BrdU^{+}$ cells in the CND of $Yap^{ND-/-}$ embryos (n=10 CNDs for each genotype, error bars indicate s.d.; **P=0.0022) compared with controls. Scale bars: 100 µm in A-C,D-I′,J,K; 50 µm in A′-C′,M,N.

Development (2015) 142, 2696-2703 doi:10.1242/dev.122044

cloacal epithelium (*EphA4*, *EphA7*, *EphrinB2*; see Weiss et al., 2014). We looked at the expression of *Robo2*, *Gata3*, *Sprouty1*, *Raldh2*, *Ret*, *Bmp4*, *Slit2*, *Islet1*, *EphA4*, *EphA7* and *EphrinB2* by *in situ* hybridization (ISH), but did not detect any significant changes in expression between controls and *Yap* cKO (supplementary material Fig. S5; Fig. 3D-G,M,N; and data not shown). We also investigated whether *Yap* deletion from the ND affected cell polarity. Immunostaining for Crumbs3 (Crb3), E-cadherin, ZO-1 (Tjp1 – Mouse Genome Informatics) and Laminin revealed that *Yap*-depleted cells acquire apico-basal polarity like control cells (supplementary material Fig. S5P-T′). Expression of *Wnt6*, *Mal2*, *Prss8*, *Cdh16*, *Cldn4*, *Rnf128*, *Wnt9b* and *Tbx3* in the ND were unaffected by *Yap* deletion (supplementary material Fig. S5H-O′). Thus, deletion of *Yap* from the ND does not lead to obvious defects in cell polarity, adhesion or cell specification in the caudal ND.

Yap and *Taz* have partially redundant functions in urinary tract development

Our data indicate that $Yap^{ND-/-}$ mice have abnormal kidney and urinary tract morphogenesis. The *Yap* paralog *Taz* is required for proper kidney development, as *Taz* null mice have cystic kidneys (Hossain et al., 2007; Makita et al., 2008). To investigate the function of *Taz* specifically in the ND derivatives, we generated $Hoxb7{:}Cre^{tg/+}$ $Taz^{flox/flox}$ mice ($Taz^{ND-/-}$). $Taz^{ND-/-}$ kidneys were similar to controls in size, and were functional at birth, based on gross anatomical examination, histology and presence of urine in the bladder at P1 (data not shown), meaning that either *Taz* is not required for morphogenesis or that *Yap* is sufficient in the absence of *Taz*. Interestingly, we found that removal of *Taz* from the UB compartment did not lead to cyst formation, in comparison to removal of *Taz* from the condensing mesenchyme (Reginensi et al., 2013) or in $Taz^{-/-}$ embryos (Hossain et al., 2007; Makita et al., 2008), indicating that Taz function is needed in developing nephrons to prevent cyst formation.

To determine whether there is functional redundancy between *Yap* and *Taz* in the UB compartment, we generated double conditional knockout mice ($Hoxb7{:}Cre^{tg/+}$ $Yap^{flox/flox}$ $Taz^{flox/flox}$, called $Yap/Taz^{ND-/-}$). Immunostaining with an anti-Yap/Taz antibody confirmed the absence of Yap/Taz expression in the epithelial compartment of $Yap/Taz^{ND-/-}$ kidneys at E12.5 (supplementary material Fig. S6A,B). Significantly, deletion of one or two alleles (Fig. 5B and C, respectively) of *Taz* showed dramatic exacerbation of the *Yap* mutant phenotype compared with controls (Fig. 5A). Indeed, $Yap/Taz^{ND-/-}$ kidneys were severely dysplastic, with no ureters at E18.5 (Fig. 5C). Earlier (E11.25) defects seen in *Yap* cKO were aggravated by the additional deletion of *Taz*, with aberrant branching morphogenesis, blind-ending NDs and defective ND-cloaca connection (Fig. 5D-F). The dramatic defects of *Yap/Taz* double mutants were also seen earlier in development, with greatly increased apoptosis seen in TUNEL staining at E11.25 (Fig. 5G,H) and with cleaved-caspase 3 staining at E12.5 (Fig. 5I,J). Taken together, these data demonstrate that *Yap* and *Taz* play partially redundant roles in development of the urinary tract, and that this pathway is a crucial regulator of kidney and ureter development.

Ret haploinsufficiency rescues the *Yap* cKO phenotypes

Ectopic budding and ureter maturation defects are observed in cases of increased Gdnf/Ret signaling. Consistent with a potentially increased level of Ret signaling in *Yap* ND mutants, we observed increased expression of the Ret downstream targets *Crlf1*, *Sprouty1*, *Etv4* and *Etv5* in *Yap* cKO ND compared with controls at E10.5 (Fig. 6A-H). We examined expression of phospho-ERK (p-ERK), a classic indicator of Ret activity, in the ND, UB and CND. Whereas p-ERK staining levels in E10.5 ND and UB were similar in controls and *Yap* mutants (supplementary material Fig. S6C-F), we observed foci of increase p-ERK staining in the CND and ND of *Yap* mutants compared with controls at E11.5 (Fig. 6I-J″; compare J′ and J″ with I′). To test the hypothesis that the *Yap* cKO phenotype is due to increased Gdnf/Ret signaling, we reduced the gene dosage of *Ret* in *Yap*-ND null mice by using a Ret-EGFP knock-in allele (Hoshi et al., 2012). Complete deletion of *Ret* in *Yap*-ND null mice ($Ret^{-/-}$ $Yap^{ND-/-}$) led to renal agenesis or rudimentary kidneys (Fig. 6M; and data not shown), as Ret is required for UB budding. Reduced levels of Ret signaling by generating *Yap* cKO animals heterozygous for *Ret* ($Hoxb7{:}Cre^{tg/+}$ $Yap^{flox/flox}$ $Ret^{+/-}$) reduced the severity of defects in *Yap*-ND null mice. Remarkably, whereas only 9% of $Yap^{ND-/-}$ ureters were connected to the bladder at P0 (2/22 ureters, see Fig. 6L,O), 50% of $Yap^{ND-/-}$ $Ret^{+/-}$ embryos showed ureter-bladder connection (9/18 ureters, see Fig. 6N,O). Thus, simply reducing Ret signaling can partially suppress the morphological effects of loss of *Yap* in ND morphogenesis.

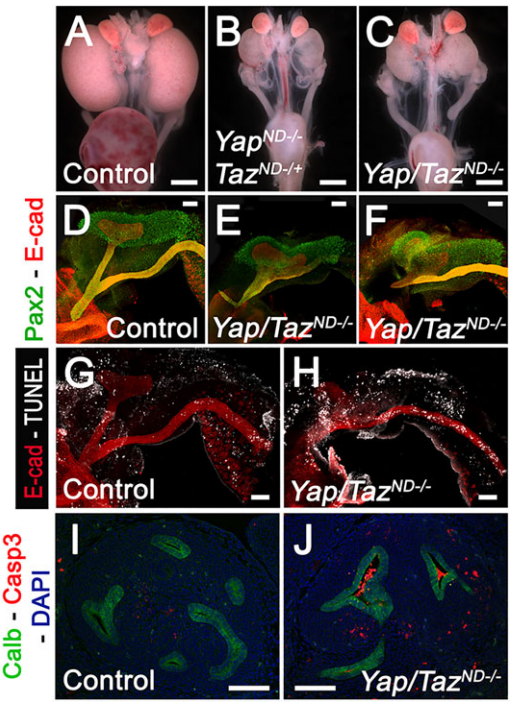

Fig. 5. *Yap* and *Taz* have partially redundant functions in urinary tract formation. Macroscopic view of the urogenital system from wild-type (A), $Yap^{ND-/-}$; $Taz^{ND+/-}$ (B) and $Yap/Taz^{ND-/-}$ (C) kidneys at P0. Note bilateral reduction in kidney size, empty bladder and the absence of ureter in the double knockout compared with control. The 'Auto Contrast' function of Photoshop was used to increase the contrast of the original pictures. Pax2/E-cadherin WM-IF staining at E11.25 revealed the extent of kidney abnormalities in *Yap*/*Taz* double mutants (E,F) compared with controls (D). TUNEL staining at E11.25 revealed strong increase in apoptotic cells in ND depleted of *Yap* and *Taz* (H) compared with controls (G). E-cadherin staining was used to visualize the ND compartment. Cleaved-caspase 3 staining at E12.5 revealed an increase in apoptosis in the ureter compartment of *Yap*/*Taz* double KO (J) compared with controls (I). Scale bars: 1 mm in A-C; 100 µm in D-J.

DISCUSSION

The navigation of the ND to the cloaca is a complex developmental process, requiring tight regulation of migration, cell polarity,

Development (2015) 142, 2696-2703 doi:10.1242/dev.122044

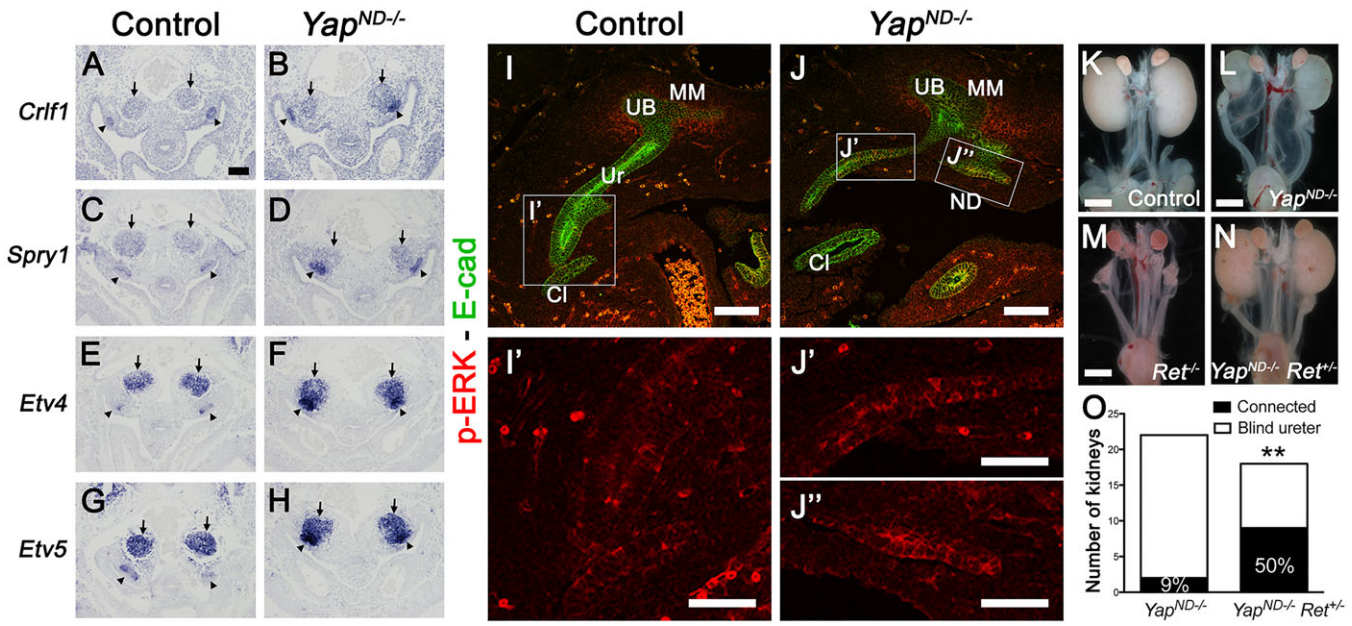

Fig. 6. Increased Ret signaling in *Yap* mutants and partial rescue of ND defects by Ret haploinsufficiency. (A-H) ISH revealed increased expression of *Crlf1*, *Sprouty1*, *Etv4* and *Etv5* expression in *Yap* mutant NDs (black arrowheads) compared with controls at E10.5. Note the apposition of the MM (arrows) on the UB (arrowheads) in *Yap* mutants, whereas both compartments are well separated in controls. (I-J″) Phospho-ERK staining in controls and *Yap* mutants at E11.5. E-cadherin counterstaining was used to label the epithelial structures. Panels J′ and J″ indicate the increased p-ERK expression in the CND (J′) and ND (J″) of *Yap* mutants compared with controls (I′). (K-N) Macroscopic views of the urogenital system from control (K), $Yap^{ND-/-}$ (L), $Ret^{-/-}$ (M) and $Yap^{ND-/-}$ $Ret^{+/-}$ (N) kidneys at P0. (O) Quantification of cases in which the ureter was connected to the bladder in controls and $Yap^{ND-/-}$ $Ret^{+/-}$ animals. Scale bars: 100 µm in A-J; 50 µm in I′-J″; 1 mm in K-N.

adhesion and apoptosis. Time-lapse imaging of the migrating ND shows growth-cone-like behavior, with multiple filopodial-like extensions sampling the environment (Chia et al., 2011). Gdnf/Ret signaling is crucial in directing the migration and budding behavior of the ND. As such, Ret signaling is known to be under multiple layers of regulation: Lim1, Pax2, Gata3, Ephrins and Raldh2 all regulate *Ret* expression or activity. In addition, activation of Ret signaling is also regulated by upstream regulators, such as Gdnf, Gfrα1, Robo2 and Bmp4, as well as modulators of downstream signaling such as Sprouty1. We add here to the already known regulators of ND behavior and Ret sensitivity the transcriptional co-regulators Yap and Taz. We show that, in the absence of *Yap*, the ND can effectively migrate to the cloaca but fails to insert, and eventually retracts, leading to hydroureter, hydronephrosis and perinatal lethality. Our genetic analysis indicates that Yap reduces sensitivity of the ND to Ret signaling, as we observed increased Ret signaling activity in the ND and a dramatic rescue of the *Yap* ND phenotype simply by removing one copy of *Ret*. These genetic data imply that Yap functions as a modifier of RET in human CAKUT.

Increased sensitivity to Ret signaling is also a characteristic of *Sprouty1* mutants, as shown by the presence of ectopic budding *Sprouty1*-deficient embryos. However, we did not detect a loss of *Sprouty1* expression in *Yap* ND mutants. Excess Raldh2 or Gata3 could also lead to increased *Ret* expression, but no obvious expression change for these genes was seen in *Yap* ND mutants. As *Ret* expression is also not obviously affected in *Yap*-deficient embryos, our results suggest that Yap regulates Ret pathway activity rather than *Ret* expression. Because the *Hoxb7:Cre* line only removes *Yap* from the ND cells, this also suggests that the changes in Ret signaling are due to cell-autonomous effects.

Ret signaling in the kidney is activated by the formation of a receptor complex with the glial cell-derived neurotrophic factor (Gdnf) and its co-receptor Gfrα1. Activation of Ret results in phosphorylation of major docking-site tyrosine (Y) residues in the cytoplasmic domain of Ret, activating several downstream signaling pathways, including PLCγ, SRC, PI3K and MAPK. Loss of *Ret* leads to loss of caudal migration of the ND (Chia et al., 2011). Mutation of the different docking-site tyrosines on Ret can differentially activate subsets of downstream pathways (Jain et al., 2010). Ret Y1015 serves as the docking site for PLCγ, whereas RetY1062 is the docking site for activation of the Ras/MAPK and PI3K pathways in the urinary tract (Davis et al., 2014).

Comparison of the $Yap^{ND-/-}$ phenotype with different *Ret* mutants provide hints as to how Yap might act to repress Ret signaling. Previous studies have shown that mutation of *RetY1015* leads to a complex CAKUT phenotype that resembles that of *Yap* cKO ND, whereas loss of Ret or mutation of *RetY1062* leads to kidney agenesis or rudimentary kidneys. $Yap^{ND-/-}$ mutants show many similarities to Ret^{Y1015} mutants, such as abnormal localization of the MM (supplementary material Fig. S6G,H), an abnormally extended CND with increased proliferation, and ectopic budding leading to multiplex kidneys with hydroureter. However, the $Yap^{ND-/-}$ and Ret^{Y1015} phenotypes also show some major differences; for example, the ectopic buds in *Yap* ND mutants are less anteriorly placed than in Ret^{Y1015} mutants, and *Ret* mutants have elongated CNDs due to decreased apoptosis. In addition, the ND in Ret^{Y1015F} mutants remains adhered to the bladder and does not show the blind-ending phenotype seen in *Yap* mutants. Thus, whereas we have shown that loss of *Yap* sensitizes to Ret signaling, there are aspects of the ND-cloacal morphogenesis that are Ret-independent.

The *Yap* mutant ND detaches from the cloaca while it is still elongating, and displays increased proliferation. Coexistence of these two observations might seem contradictory; however, it is

Development (2015) 142, 2696-2703 doi:10.1242/dev.122044

tempting to speculate that proper insertion of the ND into the cloaca is required to initiate decreased proliferation in the CND, and for further ureter-bladder remodeling.

We observed changes in the epithelial organization of the *Yap* mutant ND. Whereas the CND is a pseudo-stratified epithelium in wild-type embryos, the *Yap*-depleted CND and ureter is a single layer epithelium (supplementary material Fig. S4F-K). As YAP is known in many systems to promote proliferation, this might contribute to these morphological differences.

In summary, we have shown here that loss of *Yap* and *Taz* lead to dramatic defects in the mouse urinary tract that resemble human CAKUT, and our data suggest that mutations in the Hippo pathway are a cause of CAKUT. In addition, our study shows that lower urinary tract defects induced by loss of *Yap* can be suppressed by reduction in *Ret* gene dosage. Up to 5% of CAKUT have *RET* mutations, and our data support the notion that the Hippo pathway might directly or indirectly modify the outcome or features of CAKUT in patients with *RET* mutations. These findings may have broader implications, as the RET pathway is modulated by both upstream and downstream regulators of kidney and urinary tract development that have been independently shown to be important in patients with CAKUT. These studies have implications for the understanding of CAKUT in humans; they suggest that CAKUT, induced by defects in the Hippo pathway, is modified by treatment with Ret inhibitors.

MATERIALS AND METHODS

Mouse lines

The *Hoxb7:Cre*$^{tg/+}$, *Taz*^{flox}, *Yap*^{flox} and *Ret*$^{EGFP/+}$ mouse strains have been described elsewhere (Zhao et al., 2004; Reginensi et al., 2013; Hoshi et al., 2012, respectively). All mice were maintained on a mixed genetic background. Husbandry and ethical handling of mice were conducted according to guidelines approved by the Canadian Council on Animal Care. Genotyping was performed by PCR using genomic DNA prepared from mouse ear punches.

Histological and immunological analyses

Embryonic samples from timed matings (day of vaginal plug=E0.5) were collected, fixed in 4% paraformaldehyde overnight (O/N) at 4°C, serially dehydrated and then embedded in paraffin. Microtome sections of 7 µm thickness were examined histologically via periodic acid-Schiff staining. For immunofluorescent analysis, paraffin sections were de-waxed and rehydrated via ethanol series. Antigen retrieval was performed by boiling the sections for 20 min in Antigen Unmasking Solution (H-3300, Vector Laboratories). Sections were incubated for 1 h in blocking solution (3% BSA, 10% goat serum, 0.1% Tween 20 in PBS) at room temperature (RT). Blocking solution was replaced by a solution of primary antibodies diluted in 3% BSA, 3% goat serum and 0.1% Tween 20 in PBS. The following primary antibodies were used in this study: anti-α-SMA (A7607, Sigma; 1/200), anti-Calbindin (PC253C, Calbiochem; 1/300), anti-Cleaved-caspase 3 (#9661, Cell Signaling Technology; 1/200), anti-Crumbs3 (HPA013835, Sigma Prestige Antibodies; 1/300), anti-E-cadherin (Mouse, 610181, BD Transduction Laboratories; 1/300), anti-E-cadherin (Rabbit, #3195, Cell Signaling Technology; 1/300), anti-Laminin (L9393, Sigma; 1/300), anti-Pax2 (PRB-276P, Covance; 1/300), anti-Phospho-Yap (#4911, Cell Signaling Technology; 1/150), anti-Yap (sc-101199, Santa Cruz Biotechnology; 1/50-1/150), anti-Yap/Taz (#8418, Cell Signaling Technology; 1/150) and anti-ZO-1 (Invitrogen; 1/100). Relevant Cy3- or FITC-conjugated secondary antibodies (Jackson Laboratories) were used for primary antibody detection. Slides were mounted using Vectashield with or without DAPI (Vector Laboratories). Fluorescent images were taken with a Nikon C1 plus Digital Eclipse confocal microscope. For immunohistochemistry, the same procedure was used, with the addition of one step after the rehydration. Slides were immersed in 3% H_2O_2 in PBS for 20 min to block endogenous peroxidases. The anti-Yap/Taz antibody was incubated for 48 h at 4°C. Then, undiluted secondary antibody (EnvisionPlus from Dako) was applied to the sections for 1 h at RT. Samples were washed, developed with DAB, counterstained with hematoxylin and mounted in pertex.

Whole-mount immunofluorescence

Embryos were dissected at suitable timepoints and fixed in 4% PFA/PBS (pH 7.4) at 4°C O/N, then rinsed with PBS at RT several times. Urinary tracts were dissected under the microscope, soaked in PBS-BB (1% BSA/0.2% skim milk/0.3% Triton X-100/1× PBS) as a blocking solution and incubated O/N at 4°C on a shaker (Hoshi et al., 2012). Tissues were incubated with primary antibody (anti-Pax2, PRB-276P, Covance; 1/200; and anti-E-cadherin, AF748, R&D Systems; 1/50) solution appropriately diluted with PBS-BB at 4°C O/N, then washed with PBS-Tr (0.3% Triton X-100/1× PBS) twice at RT for one or two hours and once at 4°C O/N on a shaker. They were then incubated with secondary antibody solution appropriately diluted with PBS-BB O/N at 4°C, washed in PBS-Tr a few times at RT, and samples were imaged in 50% Glycerol/1× PBS with Nikon C1 confocal system with NIS Elements software (Nikon Instruments).

Whole-mount TUNEL staining (with whole-mount immunofluorescence)

After whole-mount immunofluorescence with anti-E-cadherin antibody, specimens were rinsed three times with PBS-Tr and incubated with 1× TdT buffer (130 mM sodium cacodylate/1 mM cobalt chloride/30 mM Tris-Cl, pH 7.4/0.1% Triton X-100). This was followed by 1-2 h incubation in the TdT buffer (adjusted pH to 7.2 with HCl) at RT. The samples were then treated with TdT reaction buffer (250 units TdT, #03333566001, Roche/1 nmol biotin-conjugated dUTP, #11093070910, Roche, in 1 ml 1× TdT buffer) O/N at RT on a shaker to label apoptotic cells. TUNEL-positive cells were visualized after incubation of labeled specimens with DyLight TM 649-conjugated streptavidin (016-490-084, Jackson ImmunoResearch) diluted 1:400 with 1× PBS/5% BSA/0.3% Triton X-100. Signals were visualized and photographed with Nikon C1 confocal system using NIS Elements software (Nikon Instruments; Hoshi et al., 2012).

BrdU incorporation

BrdU solution containing 5-Bromo-2′-deoxyuridine (10 mg/ml) was injected intraperitoneally in pregnant mice (50 mg BrdU/kg body weight) 1 h before embryonic dissection. The samples were prepared and sectioned as described above before overnight incubation with anti-mouse BrdU antibody (Clone Bu20a, Dako; 1/300).

Intrapelvic dye injections

Royal Blue ink (Pelikan) solution was injected into the renal pelvis of isolated whole-urogenital system at E18.5 using a pulled-out Pasteur glass pipette. Pressure was applied to push the ink from the pelvis to the bladder.

In situ hybridization

Embryos were fixed in 4% paraformaldehyde in PBS O/N at 4°C and then paraffin-embedded. Further processing of the embryos and ISH were carried out as described (Wilkinson and Nieto, 1993). Riboprobes were obtained from Open Freezer at the Lunenfeld–Tanenbaum Research Institute (Toronto, Canada) (Olhovsky et al., 2011).

Measurement of common ND length

E11.5 embryos were sectioned sagittally and used for quantification of CND length. Length of the CND was calculated as the length from the ureter-ND junction to the cloaca epithelium (red line in Fig. 3G,I). If the ND was detached from the cloaca in *Yap* mutants, the length was measured from the ureter-ND junction to the tip of the ND (red line in Fig. 3H). Quantification of the CND length at E12.5 was performed using the WM-IF images as in supplementary material Fig. S3C-E.

Whole-mount X-Gal staining

Embryos were fixed in 0.2% glutaraldehyde in 0.1 M phosphate buffer, 2 mM $MgCl_2$ and 5 mM EGTA for 35 min and processed as described (Hogan et al., 1994).

Development (2015) 142, 2696-2703 doi:10.1242/dev.122044

Statistical analyses

All data are expressed as mean values with standard deviation (s.d.). An unpaired two-tailed *t*-test was used to determine differences between two groups (e.g. wild type versus mutant). All statistical analyses were conducted using GraphPad Prism 5.0a software.

Acknowledgements

We thank Carlton Bates (Children's Hospital of Pittsburgh) and Jeff Wrana (Lunenfeld–Tanenbaum Research Institute, Toronto) for the *Hoxb7:Cre*$^{fg/+}$ and *Yap*/*Taz flox* mouse lines, respectively.

Competing interests

The authors declare no competing or financial interests.

Author contributions

A.R. carried out all the experiments unless stated otherwise. S.K.B. and M.B. performed the TUNEL analysis at E12. M.H. and S.J. performed whole-mount 3D confocal microscopy, including ND-cloaca joining, MM disposition, WM-IF (E10.5, E11.5) and TUNEL analysis. A.R. and H.M. analyzed the data and wrote the manuscript.

Funding

This work was supported in part by grants from the Canadian Institutes of Health Research [MOP 136924, 84468] and by Cell Lineage and Differentiation Research [Grant No. 1-FY11-506] from the March of Dimes Foundation to H.M., and by National Institutes of Health [DK082531] and Washington University Kidney Translational Research Core [DK079333] to S.J. Deposited in PMC for release after 12 months.

Supplementary material

Supplementary material available online at
http://dev.biologists.org/lookup/suppl/doi:10.1242/dev.122044/-/DC1

References

Airik, R., Bussen, M., Singh, M. K., Petry, M. and Kispert, A. (2006). Tbx18 regulates the development of the ureteral mesenchyme. *J. Clin. Invest.* **116**, 663-674.

Basson, M. A., Akbulut, S., Watson-Johnson, J., Simon, R., Carroll, T. J., Shakya, R., Gross, I., Martin, G. R., Lufkin, T., McMahon, A. P. et al. (2005). Sprouty1 is a critical regulator of GDNF/RET-mediated kidney induction. *Dev. Cell* **8**, 229-239.

Batourina, E., Choi, C., Paragas, N., Bello, N., Hensle, T., Costantini, F. D., Schuchardt, A., Bacallao, R. L. and Mendelsohn, C. L. (2002). Distal ureter morphogenesis depends on epithelial cell remodeling mediated by vitamin A and Ret. *Nat. Genet.* **32**, 109-115.

Batourina, E., Tsai, S., Lambert, S., Sprenkle, P., Viana, R., Dutta, S., Hensle, T., Wang, F., Niederreither, K., McMahon, A. P. et al. (2005). Apoptosis induced by vitamin A signaling is crucial for connecting the ureters to the bladder. *Nat. Genet.* **37**, 1082-1089.

Chia, I., Grote, D., Marcotte, M., Batourina, E., Mendelsohn, C. and Bouchard, M. (2011). Nephric duct insertion is a crucial step in urinary tract maturation that is regulated by a Gata3-Raldh2-Ret molecular network in mice. *Development* **138**, 2089-2097.

Davis, T. K., Hoshi, M. and Jain, S. (2014). To bud or not to bud: the RET perspective in CAKUT. *Pediatr. Nephrol.* **29**, 597-608.

Grieshammer, U., Le, M., Plump, A. S., Wang, F., Tessier-Lavigne, M. and Martin, G. R. (2004). SLIT2-mediated ROBO2 signaling restricts kidney induction to a single site. *Dev. Cell* **6**, 709-717.

Halder, G. and Johnson, R. L. (2011). Hippo signaling: growth control and beyond. *Development* **138**, 9-22.

Harvey, K. and Tapon, N. (2007). The Salvador–Warts–Hippo pathway — an emerging tumour-suppressor network. *Nat. Rev. Cancer* **7**, 182-191.

Hogan, B. L., Beddington, R. S., Constantini, F. and Lacy, E. (1994). *Manipulating the Mouse Embryo*. Cold Spring Harbor: Cold Spring Harbor Laboratory Press.

Hoshi, M., Batourina, E., Mendelsohn, C. and Jain, S. (2012). Novel mechanisms of early upper and lower urinary tract patterning regulated by RetY1015 docking tyrosine in mice. *Development* **139**, 2405-2415.

Hoshino, T., Shimizu, R., Ohmori, S., Nagano, M., Pan, X., Ohneda, O., Khandekar, M., Yamamoto, M., Lim, K.-C. and Engel, J. D. (2008). Reduced BMP4 abundance in Gata2 hypomorphic mutant mice result in uropathies resembling human CAKUT. *Genes Cells* **13**, 159-170.

Hossain, Z., Ali, S. M., Ko, H. L., Xu, J., Ng, C. P., Guo, K., Qi, Z., Ponniah, S., Hong, W. and Hunziker, W. (2007). Glomerulocystic kidney disease in mice with a targeted inactivation of Wwtr1. *Proc. Natl. Acad. Sci. USA* **104**, 1631-1636.

Iizuka-Kogo, A., Ishidao, T., Akiyama, T. and Senda, T. (2007). Abnormal development of urogenital organs in Dlgh1-deficient mice. *Development* **134**, 1799-1807.

Jain, S., Encinas, M., Johnson, E. M., Jr. and Milbrandt, J. (2006). Critical and distinct roles for key RET tyrosine docking sites in renal development. *Genes Dev.* **20**, 321-333.

Jain, S., Knoten, A., Hoshi, M., Wang, H., Vohra, B., Heuckeroth, R. O. and Milbrandt, J. (2010). Organotypic specificity of key RET adaptor-docking sites in the pathogenesis of neurocristopathies and renal malformations in mice. *J. Clin. Invest.* **120**, 2405-2415.

Kaku, Y., Ohmori, T., Kudo, K., Fujimura, S., Suzuki, K., Evans, S. M., Kawakami, Y. and Nishinakamura, R. (2013). Islet1 deletion causes kidney agenesis and hydroureter resembling CAKUT. *J. Am. Soc. Nephrol.* **24**, 1242-1249.

Makita, R., Uchijima, Y., Nishiyama, K., Amano, T., Chen, Q., Takeuchi, T., Mitani, A., Nagase, T., Yatomi, Y., Aburatani, H. et al. (2008). Multiple renal cysts, urinary concentration defects, and pulmonary emphysematous changes in mice lacking TAZ. *Am. J. Physiol. Renal. Physiol.* **294**, F542-F553.

Miyazaki, Y., Oshima, K., Fogo, A., Hogan, B. L. M. and Ichikawa, I. (2000). Bone morphogenetic protein 4 regulates the budding site and elongation of the mouse ureter. *J. Clin. Invest.* **105**, 863-873.

Morin-Kensicki, E. M., Boone, B. N., Howell, M., Stonebraker, J. R., Teed, J., Alb, J. G., Magnuson, T. R., O'Neal, W. and Milgram, S. L. (2006). Defects in yolk sac vasculogenesis, chorioallantoic fusion, and embryonic axis elongation in mice with targeted disruption of Yap65. *Mol. Cell. Biol.* **26**, 77-87.

Olhovsky, M., Williton, K., Dai, A. Y., Pasculescu, A., Lee, J. P., Goudreault, M., Wells, C. D., Park, J. G., Gingras, A.-C., Linding, R. et al. (2011). OpenFreezer: a reagent information management software system. *Nat. Methods* **8**, 612-613.

Pan, D. (2010). The hippo signaling pathway in development and cancer. *Dev. Cell* **19**, 491-505.

Reginensi, A., Scott, R. P., Gregorieff, A., Bagherie-Lachidan, M., Chung, C., Lim, D.-S., Pawson, T., Wrana, J. and McNeill, H. (2013). Yap- and Cdc42-dependent nephrogenesis and morphogenesis during mouse kidney development. *PLoS Genet.* **9**, e1003380.

Schedl, A. (2007). Renal abnormalities and their developmental origin. *Nat. Rev. Genet.* **8**, 791-802.

Staley, B. K. and Irvine, K. D. (2012). Hippo signaling in Drosophila: recent advances and insights. *Dev. Dyn.* **241**, 3-15.

Uetani, N. and Bouchard, M. (2009). Plumbing in the embryo: developmental defects of the urinary tracts. *Clin. Genet.* **75**, 307-317.

Uetani, N., Bertozzi, K., Chagnon, M. J., Hendriks, W., Tremblay, M. L. and Bouchard, M. (2009). Maturation of ureter-bladder connection in mice is controlled by LAR family receptor protein tyrosine phosphatases. *J. Clin. Invest.* **119**, 924-935.

Weiss, A.-C., Airik, R., Bohnenpoll, T., Greulich, F., Foik, A., Trowe, M.-O., Rudat, C., Costantini, F., Adams, R. H. and Kispert, A. (2014). Nephric duct insertion requires EphA4/EphA7 signaling from the pericloacal mesenchyme. *Development* **141**, 3420-3430.

Wilkinson, D. G. and Nieto, M. A. (1993). Detection of messenger RNA by in situ hybridization to tissue sections and whole mounts. *Methods Enzymol.* **225**, 361-373.

Zhao, H., Kegg, H., Grady, S., Truong, H.-T., Robinson, M. L., Baum, M. and Bates, C. M. (2004). Role of fibroblast growth factor receptors 1 and 2 in the ureteric bud. *Dev. Biol.* **276**, 403-415.

Zhao, B., Lei, Q.-Y. and Guan, K.-L. (2008). The Hippo–YAP pathway: new connections between regulation of organ size and cancer. *Curr. Opin. Cell Biol.* **20**, 638-646.

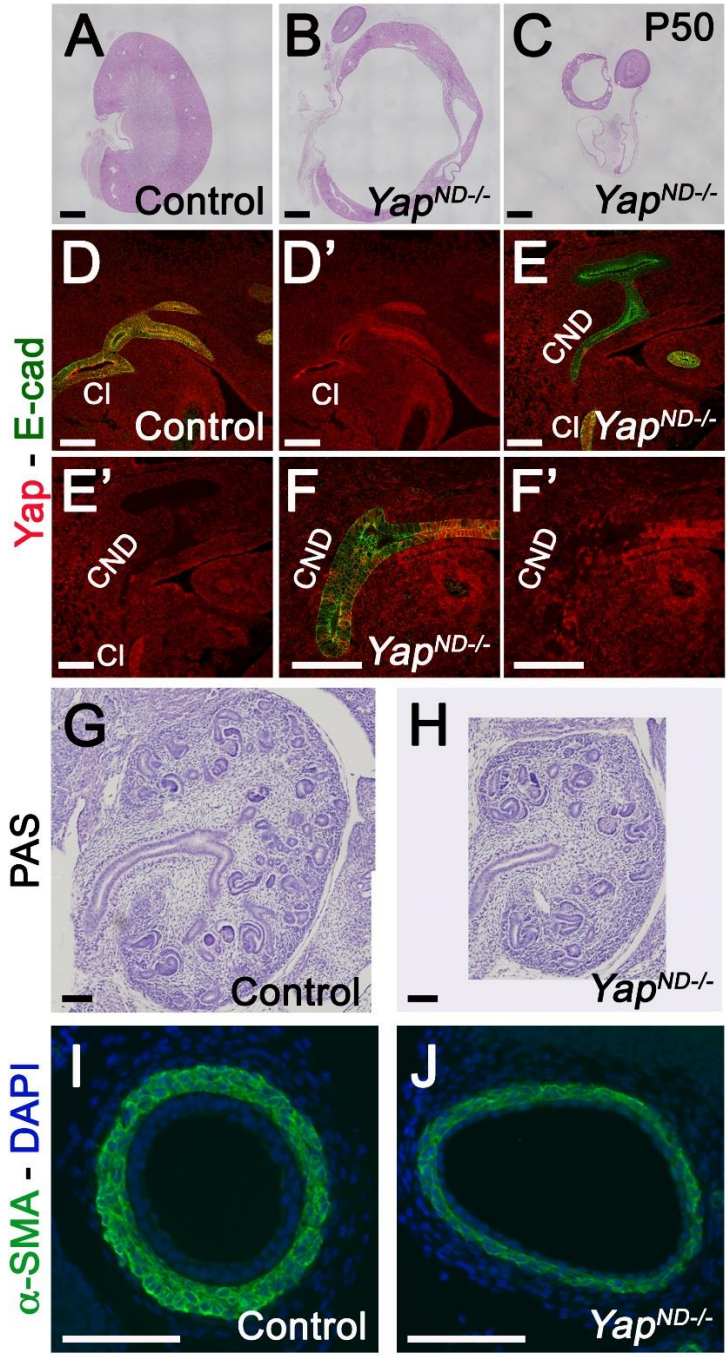

Figure S1: *Yap*$^{ND-/-}$ escapers, Cre efficiency and smooth muscle differentiation.
PAS staining of wild-type (A) and *Yap* mutant (B,C) kidneys at post-natal day 50. (D-F') Efficiency of the *Hoxb7:Cre* deletion on *Yap* conditional allele at E11.5. Yap antibody staining in controls (D) and *Yap* mutants (E) confirmed Yap deletion within the ND, UB and UB tips, whereas Yap staining in the cloaca (Cl) compartment persists. (F) Rarely, we observed mosaic efficiency of Cre deletion in the CND and the ureter which could explain why a few *Yap* cKO embryos can survive after birth. (G,H) PAS staining of E14.5 kidneys from wild-type and *Yap*$^{ND-/-}$ animals. (I,J) Alpha-smooth muscle actin immunostaining analysis on ureter cross-section of E16.5 animals showed normal differentiation of the smooth muscle along the ureter in both genotypes. Scale bars represent 1 mm (A-C) and 100 μm (D-J).

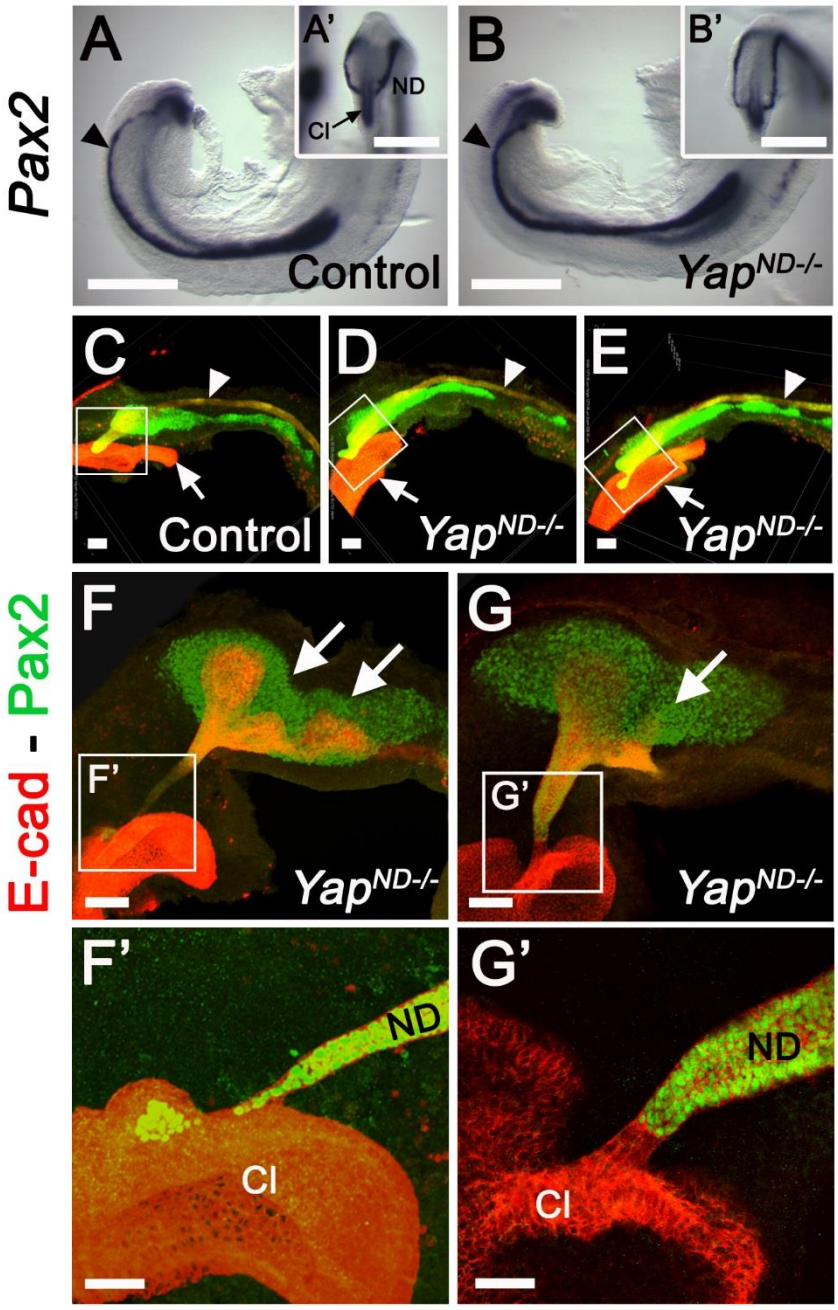

Figure S2: *Yap* signaling is essential for the ND insertion into the cloaca.
(A,B) WM ISH using *Pax2* riboprobe to visualize both ND and cloaca at E9.5 showed normal migration of the ND towards the cloaca in both genotypes. (C-E) Low magnification views of the ND - cloaca connection at E10.5 (shown in Fig. 2B-D). Arrowheads point to the ND and arrows to the cloaca. (F-G') Pax2/E-cadherin WM IF staining at E11.5 revealed the extent of the ND - cloaca connection in *Yap* mutants compared to controls. Scale bars represent 500 μm (A,B), 100 μm (C-G) and 50 μm

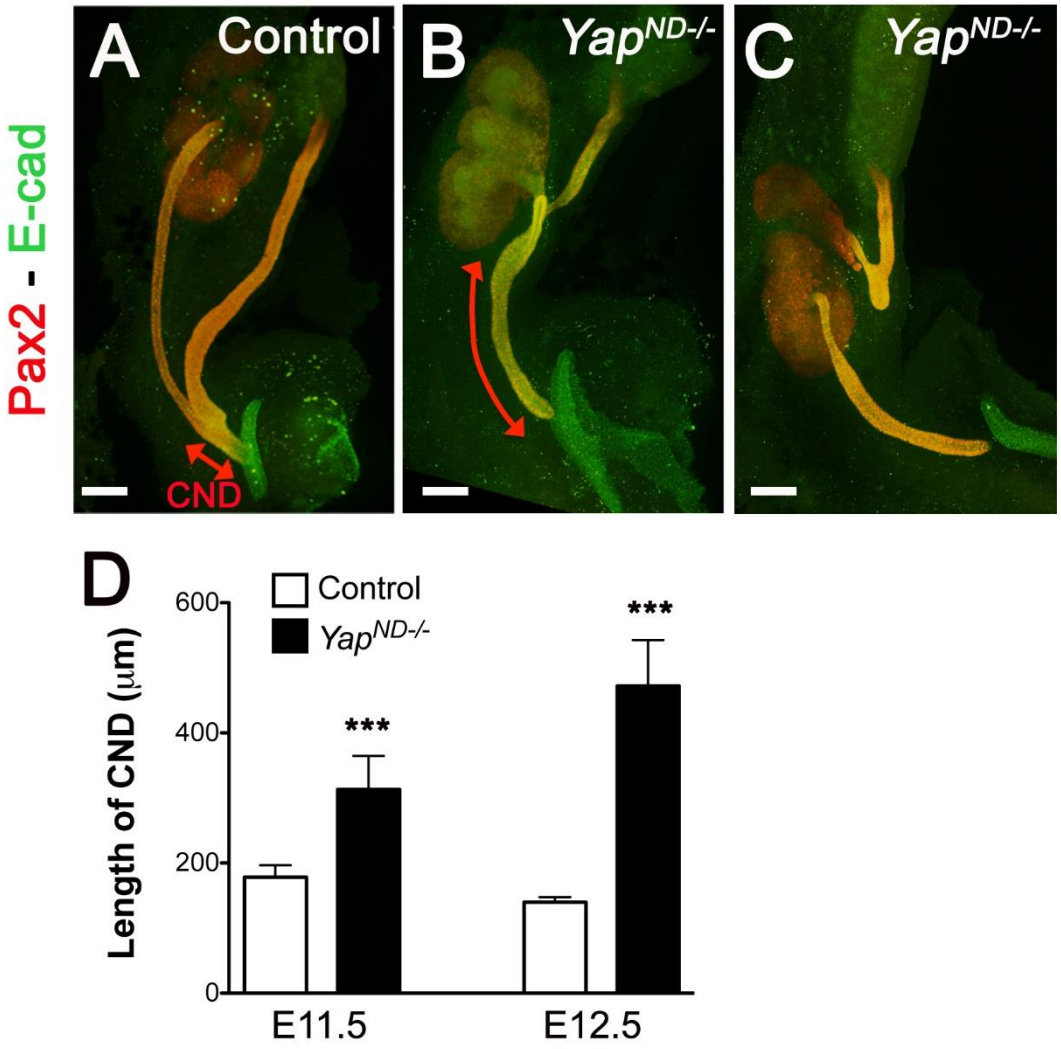

Figure S3: Increased CND length in *Yap* mutants.
(A-C) Pax2/E-cadherin WM IF staining at E12.5 revealed the extent of kidney abnormalities in *Yap* mutants compared to controls. (D) Quantification of the length of the CND at E11.5 and E12.5 in controls (white) and *Yap* mutants (black). Error bars indicate the Standard Deviation (SD). ***: $p<0.0001$. Scale bars represent 100 μm. (F',G').

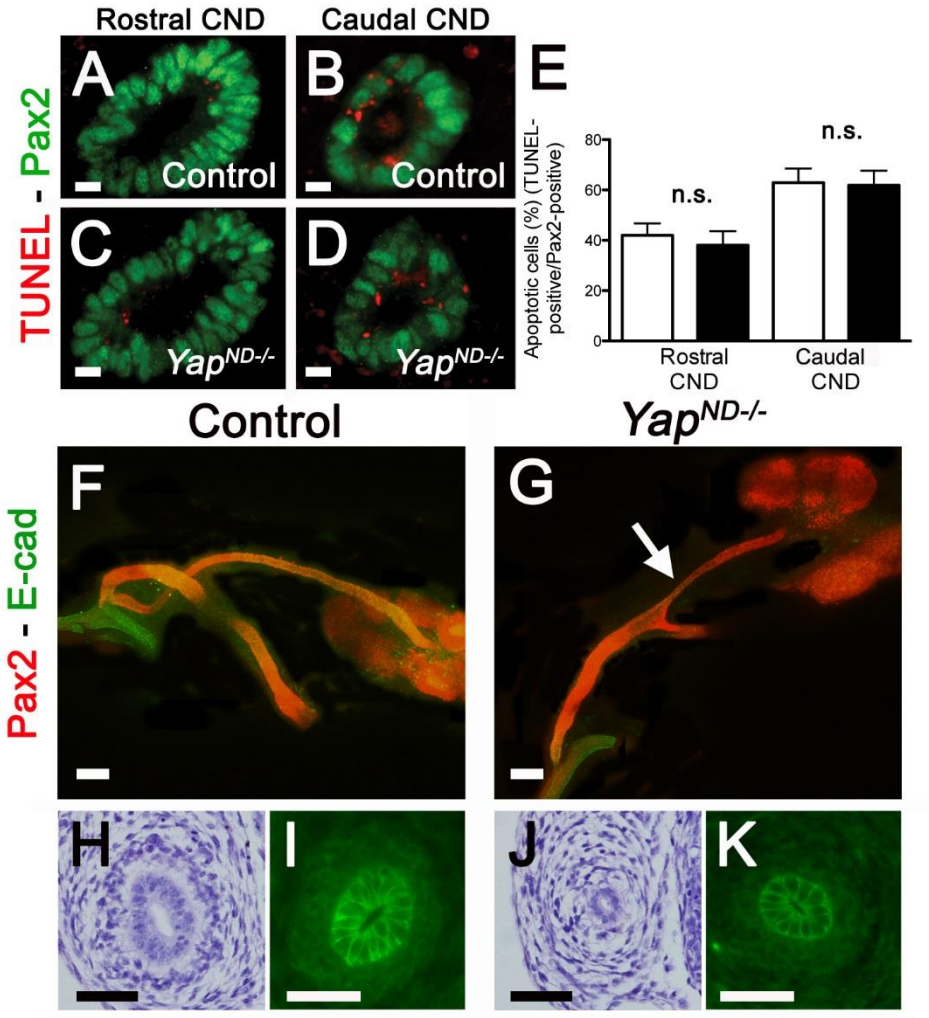

Figure S4: Altered morphology of the ureter in *Yap* mutants.
(A-D) TUNEL (red) and Pax2 (green) staining on E12.5 transverse sections of rostral CND (closest to ureter) and caudal CND (closest to bladder) of controls and *Yap* mutants. (E) Quantitative analysis of the cell death observed in control and *Yap* mutant CNDs at E12 revealed no significant (n.s.) changes. (F,G) Pax2/E-cadherin WM IF at E12.5 revealed thinning of the ureter diameter (arrow in G). This is confirmed by PAS staining (H,J) and E-cadherin (I,K) staining of ureter cross-sections at E14.5. Scale bars represent 10 μm (A-D), 100 μm (F,G) and 50 μm (H-K).

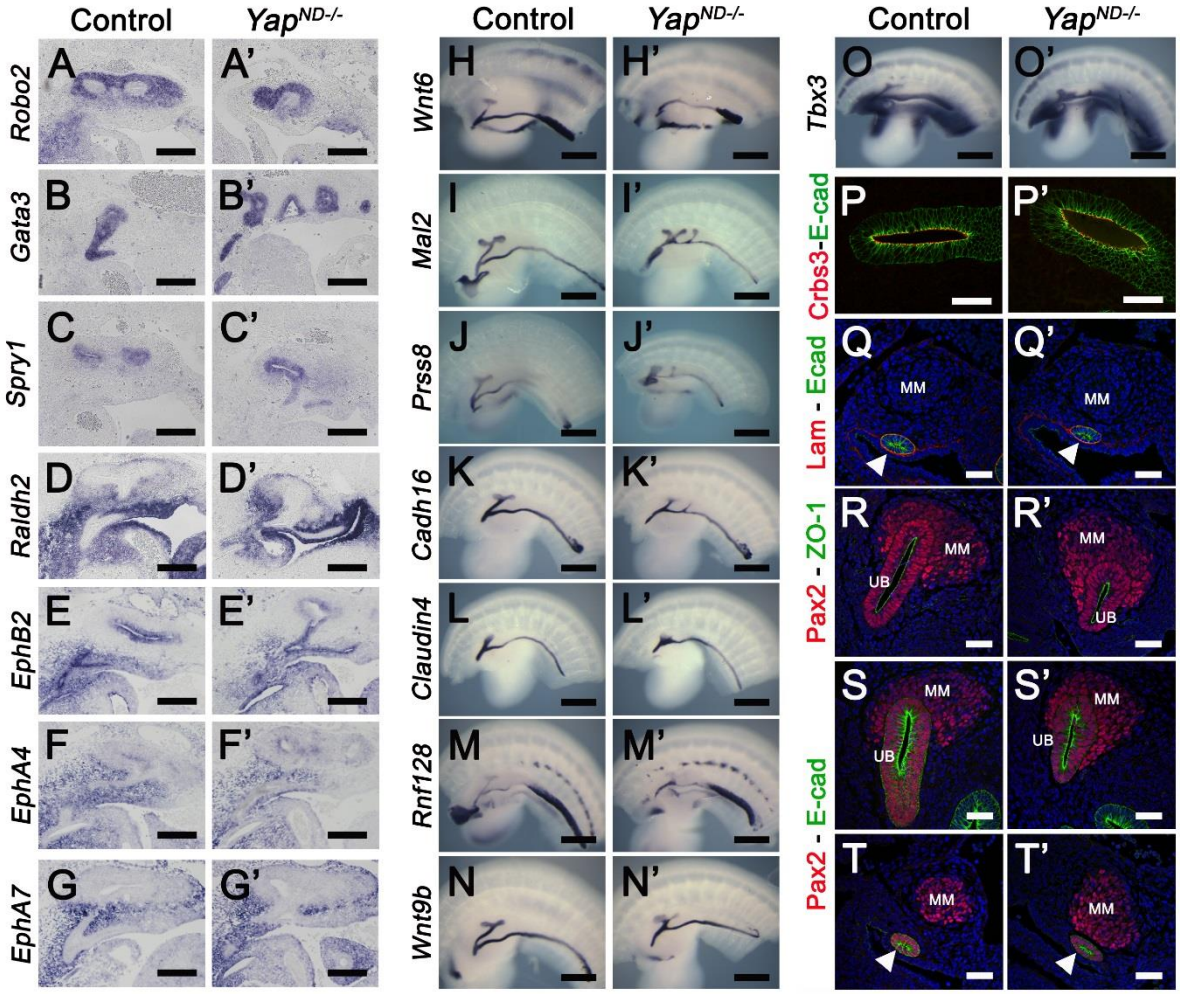

Figure S5: Cell polarity and specification is not affected by *Yap* deletion.
(A-G') *In situ* hybridization on sections showed no change in *Robo2*, *Gata3*, *Sprouty1*, *Raldh2*, *EphB2*, *EphA4* and *EphA7* expression between controls and *Yap* mutants at E11.5. (H-O') WM ISH showed normal expression of *Wnt6*, *Mal2*, *Prss8*, *Cadherin16*, *Claudin4*, *Rnf128*, *Wnt9b* and *Tbx3* in the ND of controls and mutants at E11.5. (P-T') *Yap* mutant cells, like wild-type, acquired cell polarity as shown by Crumbs3, Laminin, ZO-1 and E-cadherin staining at E10.5 (Q,T) and E11.5 (P,R,S). Scale bars represent 200 μm (A-G'), 500 μm (H-O') and 50 μm (P-T').

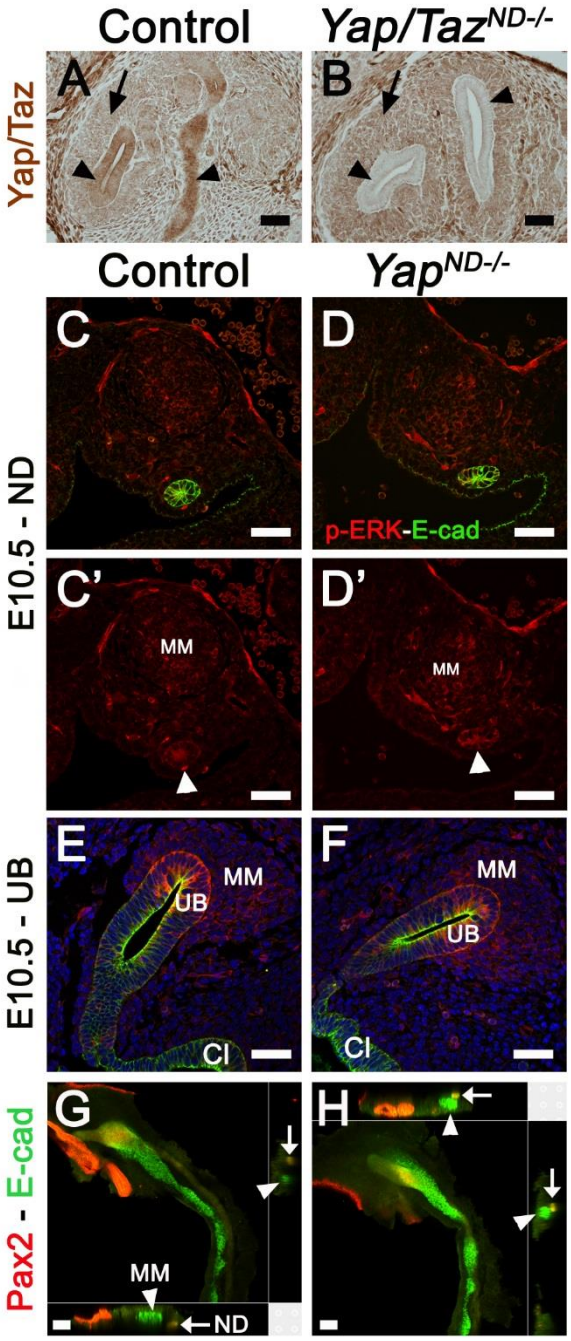

Figure S6: Efficient Cre excision of *Yap/Taz flox* alleles, p-ERK analysis and abnormal mesenchymal disposition.
(A,B) Immunostaining at E12.5 with a Yap/Taz antibody confirmed the absence of Yap/Taz expression in the ureter/UB compartment (arrowhead) of *Yap/Taz* double knockout while expression in the mesenchyme persists (arrow). (C-F) Phospho-ERK staining in controls and *Yap* mutants in the ND and UB at E10.5 and E11.5. E-cadherin counterstaining was used to label the epithelial structures. (G,H) Metanephric mesenchyme is malpositioned in *Yap* mutants. Insets represent 3D cross-sectional renderings of confocal images displayed on two axes clearly depicting the close apposition of the MM (arrowhead) and ND (arrow) in $Yap^{ND-/-}$ mutants compared to controls. ND: nephric duct, Cl: cloaca, UB: ureteric bud, MM: metanephric mesenchyme. Scale bars represent 50 μm (A-F) and 100 μm (G,H).